Hindawi
Advances in Materials Science and Engineering
Volume 2019, Article ID 3864765, 9 pages
https://doi.org/10.1155/2019/3864765

Research Article

Some Manifestations of Antioxidation Coating for Hot Precision Forging Gears

Dongcheng Li ,[1,2] Nana Han,[1] Luca Quagliato,[3] Naksoo Kim,[3] and Ge Yu[2]

[1]*Roll Forging Institute, Jilin University, Changchun, China*
[2]*School of Materials Science and Engineering, Jilin University, Changchun, China*
[3]*Department of Mechanical Engineering, Sogang University, Seoul, Republic of Korea*

Correspondence should be addressed to Dongcheng Li; dcli@jlu.edu.cn

Received 21 November 2018; Revised 17 January 2019; Accepted 29 January 2019; Published 17 February 2019

Academic Editor: Michael J. Schütze

A high temperature protective coating was prepared onto the surface of 20CrMnTi steel by brushing technique, and the heated billet was subjected to hot forging. Compared with an uncoated sample, the effect of coating on high-temperature oxidation behavior of steel was investigated by scanning electron microscopy-energy dispersive spectroscopy and X-ray diffraction. Before hot forging, an oxide layer of 153 μm was formed on the surface of the uncoated sample; however, no oxide layer was formed on the surface of the coated sample. After hot forging, the thickness of scale on the surface of uncoated gear forging is 89 μm while the thickness of coating on the surface of coated gear forging is 39 μm. It is concluded that such a coating material not only enhances the dimensional accuracy but also improves the surface quality of the gear.

1. Introduction

Gears are the most important transmission parts used to transmit motion and power between two space shafts. They have some advantages of stable transmission, wide application range, etc. With the rapid development of modern manufacturing, high precision gears are required. The cold precision plastic forming, as one of the methods processing gear, has several advantages such as excellent surface quality, without subsequent mechanical machining of the tooth surface. At present, the small modulus gear is usually fabricated through cold precision plastic forming. However, there still exists a challenge in achieving gears with modulus higher than 10 processed by the cold precision plastic forming due to its large deformation resistance and non-available large tonnage forming equipment. Although the deformation resistance of the gear can be reduced by hot forging, it is inevitable that the accuracy and surface quality of gears are poor, which are caused by accuracy of tooling, thermal expansion, and high-temperature oxidation.

In a process of hot forging, resistance of deformation and friction could lead to elastic deformation, which results in dimensional deviation of the forming product. In view of forming defects in dimensional accuracy, Balendra [1] puts forward a method to improve the accuracy of forgings by a calculation or simulation to analyze the elastic deformation of a die, and the die cavity size was compensated. In order to reduce the forging defects caused by thermal expansion of forging and die, Tian et al. [2, 3] established a formula of equivalent linear expansion rate and a theorem of linear compensation of the involute tooth profile, which provided a theoretical basis for tooth profile design of the gear with a precision forging die. However, the effect of severe oxidation on the surface of the billet at high-temperature condition has not been significantly investigated in relation to the surface quality and precision of the gear.

With the aim of protecting metals from oxidation at high temperature, coating has been widely used in hot stamping. In hot stamping, in order to achieve the best protection effect at high temperature, composition of a coating used in different steel grades is different. Al_2O_3-MgO-TiO_2-CaO ceramic coating was applied to Q235B for reducing oxidation loss [4]. MgO-CaO-Al_2O_3-SiC coatings, which could be applied on high-carbon steel [5, 6], have shown a good ability of preventing steel from oxidation and decarburization. A ceramic coating was applied on low alloy steel by the slurry spraying technique [7–11]. The coating had achieved very good antioxidation effects at 1250°C. The Al_2O_3-SiO_2-Na_2O protective coating was applied to stainless steel [12, 13]. Effect of the thickness of coating on the high-temperature oxidation was investigated. When the coating thickness is 1.5 mm, protective effect is best and the burning rate of oxidation decreased by 95%. Therefore, the forming quality of low carbon steel, high carbon steel, low alloy steel, and stainless steel in the hot stamping process can be effectively improved by protection coating. The stress state has a certain effect on the oxidation layer behavior. Metal flow is relatively simple in the stamping process. However, forging is mostly used for bulk forming of bar or billet. In a process of bulk forming, the metal flow in the three-dimensional directions and the stress state is complicated. The deformation load of forging is much larger than that of sheet stamping. At present, research studies in hot forging under the protection of antioxidation coating have not been reported.

So far, precision forging at a temperature of more than 1000°C is impossible due to intense oxidation. Aims of this paper are to achieve precision forging of gear at a temperature of more than 1000°C without additional machining of the teeth. In this paper, a high-temperature protective coating, suitable for hot forging of gear, is prepared and investigated according to material properties of the blank in order to prevent the high-temperature oxidation and to improve the dimensional accuracy of forgings. After holding the sample at 1100°C for 30 min, the surface layer structure of a sample was observed by scanning electron microscope, and high-temperature oxidation resistance of the coating was analyzed. The elements distribution and phase on the surface of the sample were studied by EDX and XRD. The section structure and surface morphology of gear forgings were analyzed by scanning electron microscope. With the results of metal flow velocity and normal pressure in DEFORM-3D simulation, the predicted loads on the coating are shown.

2. Experimental

2.1. Preparation of Steel Sample. The chemical composition of 20CrMnTi used in the present study is 0.23% C, 0.97% Cr, 0.30% Si, 0.97% Mn, 0.057% Ti, 0.059% S, 0.009% P in weight percent, and Fe balanced. Samples with diameter of 10 mm, height of 15 mm and diameter of 30 mm, height of 47 mm were prepared by a wire cutting machine, respectively. Subsequently, the samples were abraded and polished on papers of SiC from 100 to 1000 meshes. After that, the samples were cleaned and rinsed in an ultrasonic alcohol bath and dried.

2.2. Preparation of the Coating. The coating powder consists of the following analytical reagents: Al_2O_3, MgO, Al, CaO, and C. The purity of the coating powder is greater than 98%. An electron balance with an accuracy of 0.0001 grams was used for weighing the content of mixed powder. The composition of the mixed powder is 1 g Al_2O_3, 1 g MgO, 0.4 g Al, 0.2 g C, and 0.03 g CaO. The particle size of the coating was nanoscale to ensure high-temperature activity. The size of the powder is about 100 nm for Al_2O_3, 500 nm for MgO, 10 μm for Al, 500 nm for C, and 500 nm for CaO. Sodium silicate was used as a binding agent, in which silica accounts for 26%. Sodium silicate with a density of 1.35 g/cm^3 is used as 8 ml. The mass ratio of the coating powders to sodium silicate in the coating slurry is 1 : 4.106. Mixture of the coating raw materials (coating power and binding agent) was stirred at 500 rpm for 3 hours by a magnetic stirrer to make sure the slurry is homogeneous. A method of brush coating was adopted to obtain a uniform film on the steel. The thickness of coating was about 0.1 mm. Then, the coated sample was dried at 60°C for 2 hours.

2.3. Experimental and Analytical Methods. To evaluate a protecting effect of coating on 20CrMnTi at high temperatures, coated and uncoated samples with a diameter of 10 mm and a height of 15 mm were heated at 1100°C for 30 min in a muffle furnace. The heated sample was air-cooled, and then, the sample was rough ground along the radial direction with 200 mesh sandpaper. The specimen was rotated 90 degrees, and the finer sandpaper was replaced when the abrasion marks were uniform. The grinding paper was used in turn with 500 and 1000 meshes. Then, the sample was cleaned with anhydrous ethanol, and then, the surface of the sample was observed. The structure and the element distribution of the steel specimen were analyzed by scanning electron microscopy (SEM) equipped with an energy dispersive spectroscopy. Changes of phases in the coating and the oxide layer were analyzed by X-ray diffraction results.

In the gear hot forging experiment, the samples with a diameter of 30 mm and a height of 47 mm were heated to 1150°C in a muffle furnace and then formed into bevel gears in a friction press. The structure and the surface morphology of the cross section of gear forgings were characterized by SEM.

In order to verify the conditions related to the material flow velocity and forming pressure acting on the material surface during the forming operation, a numerical model has been implemented in DEFORM-3D (deformation and heat transfer simulation). In the numerical simulation, the same process conditions utilized in the experiments have been utilized and are hereafter summarized.

To the top die, a boundary condition resulting in a moving speed of 750 mm/s has been applied whereas a full constraint has been applied to its bottom surface to the bottom dies. Considering the initial position of the top die, a total of 320 steps of 0.1 mm each have been utilized to subdivide the total simulation step. In order to avoid any mesh volume loss during the simulation, the volume compensation option has been utilized both during the calculation as well as during the remeshing phase.

Dies have been considered as rigid without heat transfer, due to the small duration of the forging process and to limit the computational time, whereas the billet has been meshed utilizing tetrahedron elements with the size ratio 2 for a total count of 100,000 elements.

For the solution of the numerical model, a conjugate gradient solver with the direct iteration method has been employed considering a Lagrangian incremental integration. An initial temperature equal to 350°C has been applied to the dies whereas the initial billet temperature has been set to 1150°C. Friction has been modeled by utilizing the shear friction formulation by setting the friction factor $m = 0.3$. Moreover, the convective heat transfer coefficient between workpiece and environment has been set to 0.02 N/s·mm·°C whereas the conductive heat transfer coefficient between dies and billet to 5 N/s·mm·°C. Concerning the material properties for the 20CrMnTi steel alloy, Wei and Fu [14] characterized its high-temperature behavior by means of laboratory experiments carried out at in the temperature range between 950°C and 1150°C and for strain rates equal to 0.01/s, 0.1/s, 1/s, and 5/s. The flow stress model [14] used in this simulation is

$$\sigma = \frac{1}{0.01135}\sinh^{-1}\left[\exp\frac{\ln\dot{\varepsilon} - \ln\left(2.987\cdot 10^{14}\right) + \left(\left(3.8899\cdot 10^{5}\right)/\left(8.314\cdot T\right)\right)}{5.3914}\right], \quad (1)$$

where T is the temperature and $\dot{\varepsilon}$ is the strain rate.

3. Results and Discussion

3.1. Change of Sample Surface after Heating without Stress

3.1.1. Coating Layer Structure of Sample after High Temperature Heating. Figure 1 shows the SEM picture of the cross section of uncoated and coated samples after holding 1100°C for 30 min in a furnace. As shown in Figure 1(a), the total thickness of the oxide scale is 153 μm. Basic structure of the oxide layer consists of a dense outer layer and a loose inner layer. The outer layer is dense and thin with thickness about 12.3 μm, 8% of the total thickness of the oxide scale. The inner layer is loose and thick with thickness about 140.7 μm, 92% of the total thickness of the oxide scale. After holding at high temperature, the loose layer has good bonding strength. There are obvious cracks between the loose layer and the dense layer. The dense layer is easily detached from the loose layer.

Coated samples were held at 1100°C for 30 min. The coating was sintered and the thickness was about 105 μm, which was tightly bonded to the substrate, and there was no oxide structure between the coating and the substrate, indicating that the coating was able to play a good oxidation protection effect during heating. Compared with the oxide structure, the coating structure is relatively so dense that the amount of the oxygen diffused to the substrate decreases. The carbon powder and aluminum powder in the coating surface reacts with oxygen, thus reducing the oxidation atmosphere surrounding the steel surface. The coating reduces the oxidation of the substrate.

3.1.2. Influence of Coating on the Distribution of Elements of Substrate. Figures 2 and 3 show the results of EDS mapping of the cross section of the coated and uncoated samples held at 1100°C for 30 min. As shown in Figure 2, a Si-rich region existed at the interface of the scale and the substrate on the uncoated sample. Si in steel might react with O to form SiO_2, which reacts with FeO in the scale to produce Fe_2SiO_4 or eutectic products of FeO-Fe_2SiO_4 [6, 10–12]. Therefore, fayalite might be formed at the interface of the scale and the substrate on the uncoated sample. The compact structure of fayalite can improve the oxidation resistance of steel. Meanwhile, the fayalite products strengthen the bonding strength between the scale and the steel substrate, make scale residue on the surface of substrate in subsequent processing, and reduce the surface quality of products. As the coating ingredients contain sodium silicate, the coating material contains a certain amount of Si. It can be seen from Figure 3 that Si evenly distributed in the coating, and no enrichment is observed. The results show that the coating effectively controls the enrichment of the Si element at the interface of coating and substrate, while fayalite may be formed in the coating to improve the oxidation resistance of steel. The protective effect of fayalite in the coating makes no oxide scale structure on the surface of the substrate, which reduces the oxide residue on the substrate surface and improves the surface quality of products. Fayalite also makes the coating better bonded to the substrate surface.

As shown in Figure 3, Cr is enriched at the interface of the substrate and coating on the coated sample. The oxidation of Cr will form a dense Cr_2O_3 protective oxide film, which can effectively reduce the diffusion of oxygen into the substrate. Fe element appears in the enrichment layer of Cr, which might form an Fe-Cr spinel layer. Although the oxygen diffusion resistance in the Fe-Cr spinel is much lower than that in Cr_2O_3 [7], there is still some resistance to the diffusion of oxygen to the substrate. In the uncoated sample, no enrichment layer of Cr was found. It is impossible to form a Cr_2O_3 protective film or a dense Fe-Cr spinel layer that resists to the diffusion of oxygen to the substrate. The above results show that the coating can effectively improve the oxidation resistance of the metal.

As shown in Figure 2, the content of Fe in the oxide layer of the uncoated sample is about 81% of the Fe content in the substrate. With increasing distance from the interface of coating and substrate, the content of Fe in the coating decreases as shown in Figure 3. At a distance of 73 μm near to the interface of coating and substrate, the content of Fe element in the coating is about 55% of the substrate. The content of Fe element dramatically declined far away from the interface more than 73 μm. These phenomena indicated

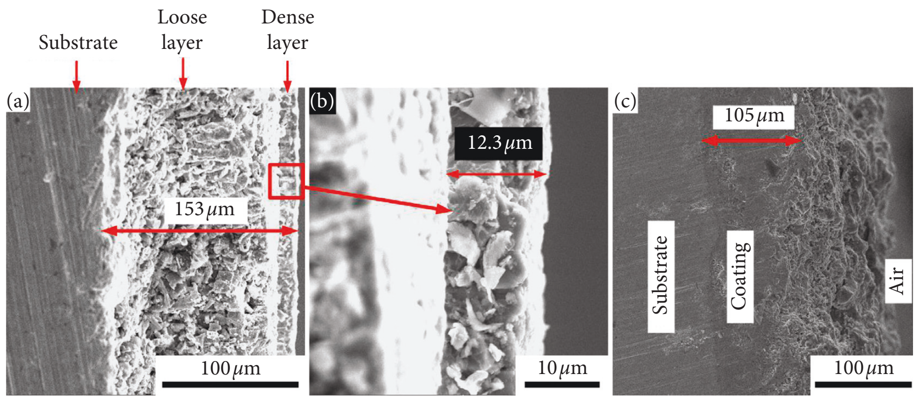

Figure 1: Cross section of the 20CrMnTi uncoated and coated samples after reheating. (a) Uncoated sample; (b) magnification of the dense layer; (c) coated sample.

that the coating creates a substance being able to resist to the diffusion of Fe during heating. Zhou et al. [11] believed a coating of MgO will react with Fe oxides to produce the Fe-Mg spinel structure when temperature rises to 820°C. The Fe-Mg spinel might be formed at a high temperature and can resist to the diffusion of Fe into the coating. The Fe-Mg spinel structure can also reduce the diffusion speed of oxygen, hinder the diffusion of oxygen into the substrate, and improve the oxidation resistance of the substance.

3.1.3. Phase Analysis of Coating Material. The XRD results of samples are shown in Figure 4. All samples were held at 1100°C for 30 min. The oxide scale of the uncoated sample was mainly composed of Fe_2O_3, Fe_3O_4, and $Fe_{2.45}Si_{0.55}O_4$ in Figure 4(a). However, in Figure 4(b), it indicates that new phases are formed on the coated sample at 1100°C, including several spinels ($MgFe_2O_4$, $MgAl_2O_4$, and $Fe(Cr,Al)_2O_4$) and ($Fe_{2.45}Si_{0.55}O_4$ and Fe_2O_3.)

At high temperature, an element of Si in the uncoated sample enriched at the interface of scale and substrate was oxidized to amorphous SiO_2. Fe_2SiO_4 was formed when the newly formed SiO_2 reacts with iron oxides according to reaction (2) [15]. Fe_2SiO_4 is unstable, and Fe^{3+} substitutes a part of Fe^{2+} and Si^{4+} in Fe_2SiO_4 through the substitution mechanism as shown in (3) [16], getting the composition $Fe_{2.45}Si_{0.55}O_4$. From Figure 4(b) it is evident that fayalite is formed in the coating. Therefore, the section structure of XRD and EDS indicated the formation of dense fayalite and spinel in the coating, which prevents the formation of the oxide scale structure on the steel surface, reduces the residual amount of oxide scale on the steel surface, and improves the surface quality of the forgings:

$$2FeO + SiO_2 \longrightarrow Fe_2SiO_4 \quad (2)$$

$$2Fe^{3+} \longrightarrow Si^{4+} + Fe^{2+} \quad (3)$$

At a lower temperature, the aluminum powder reacts with oxygen to form a dense alumina film, which can prevent the diffusion of oxygen into the metal substrate. As the temperature rises to 600°C, carbon powder in the coating reacts with oxygen, i.e., $C + O_2 = CO_2$. Oxygen content on the surface of the sample is reduced, and the oxidation of oxygen to the substrate is relieved. When the temperature rises to 800°C, the system of Na_2O-SiO_2 in sodium silicate appears in the liquid phase [17], which bonds various refractory materials (MgO, Al_2O_3, and CaO) together. It will form a dense protective film to prevent the diffusion of oxygen to the substrate. When the temperature rises to 820°C, MgO in the coating reacts with iron oxides and aluminum oxides to form a spinel structure [11]. The results of XRD and the distribution of Fe indicate that in addition to the Fe-Mg spinel structure of the $MgFe_2O_4$ component, the spinel structure of $MgAl_2O_4$ is also formed. The spinel structure increases density of the coating and effectively reduces the diffusion speed of oxygen. In EDS analysis of the coated sample, Fe was contained in the enrichment layer of Cr, indicating that Cr_2O_3 was not formed in the coating. It is further proved by XRD results that chromium reacts with iron oxides and aluminum oxides to form the $Fe(Cr,Al)_2O_4$ spinel structure above 1100°C [6], which further enhances density of the coating, inhibits the diffusion of oxygen, and improves the oxidation resistance of the sample.

3.2. Effect of Coating on Forgings

3.2.1. Effect of Coating on the Surface of Gear Forgings. The billet was heated to 1150°C and then subjected to forge in a friction press to form a certain size of bevel gear, as shown in Figures 5(a) and 5(b). After forging, a layer of material adheres to the surfaces of both coated gear forgings and uncoated gear forgings. The teeth of gears are cut out as shown in Figures 5(b) and 5(e). In Figure 5(c), after hot forging, the thickness of the scale on the surface of the uncoated gear is 89 μm, and the oxide structure is dense. In Figure 5(f), the thickness of coating on the surface of the coated gear is 39 μm, and there is no oxide structure between the coating and the substrate. The thickness of the surface residue of coated forgings is reduced by 56.2% compared with the uncoated forgings.

Figure 6 shows the gear surface after removing the coating or the scale. It can be noted that the surface of the uncoated gear is very rough; meanwhile, the surface of the

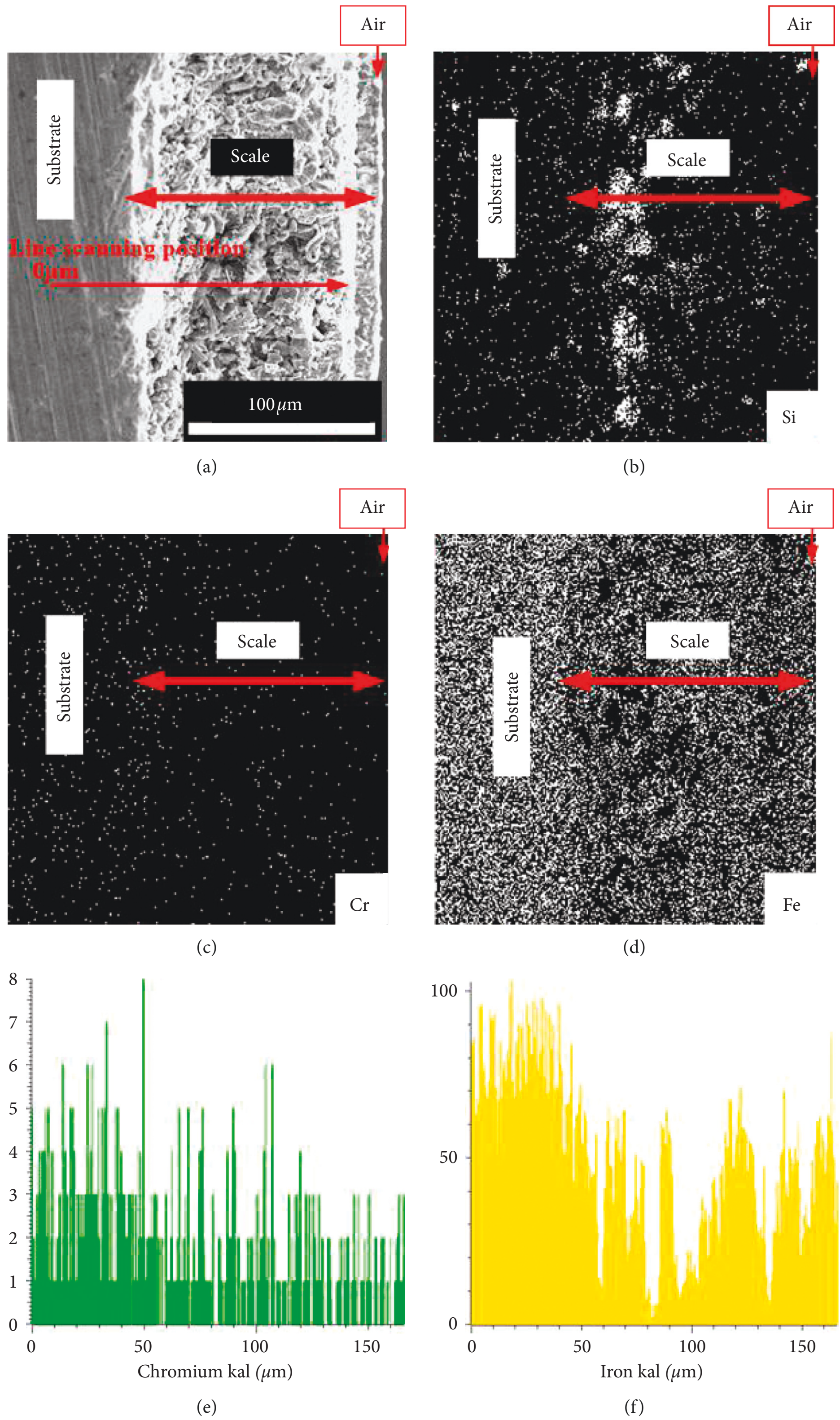

Figure 2: Element distribution on the cross section of the 20CrMnTi uncoated sample.

coated gear is very smooth. The coating can enhance the surface quality of gears. Main reason for this phenomenon is that oxidation at high temperature corrodes the surface of forging, resulting the gear surface to be rough. However, the coating reduces oxidation of the gear surface to obtain a smooth surface gear at a high temperature. When

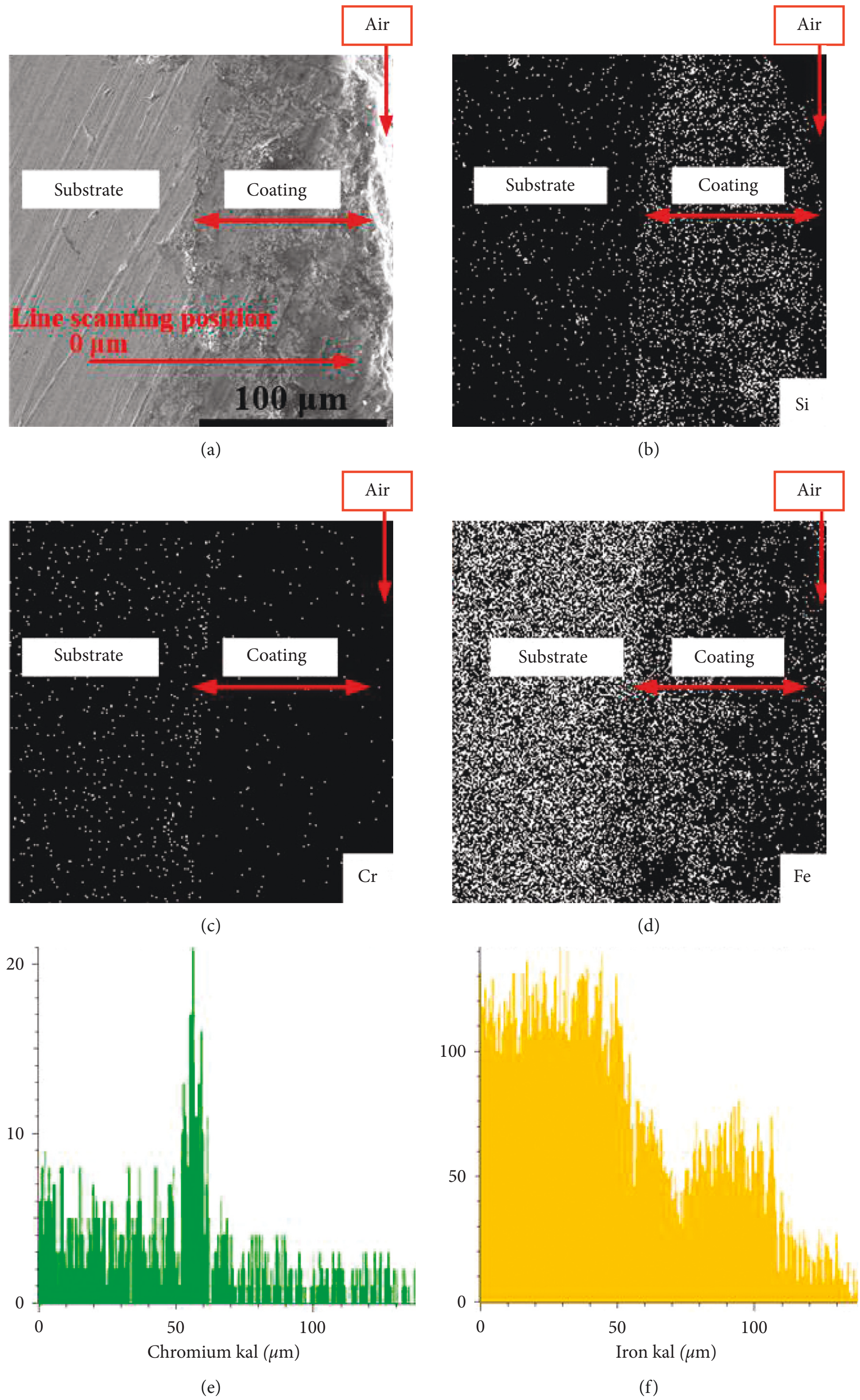

FIGURE 3: Element distribution on the cross section of the 20CrMnTi coated sample.

the coating material is applied on steel in a process of hot forging, it can not only enhance the dimensional accuracy but also improve the surface quality of gears.

3.2.2. Loads on the Surface of the Gear during Forging. After hot forging, the thickness of the scale on the surface of the uncoated gear is 89 μm and the thickness of coating on

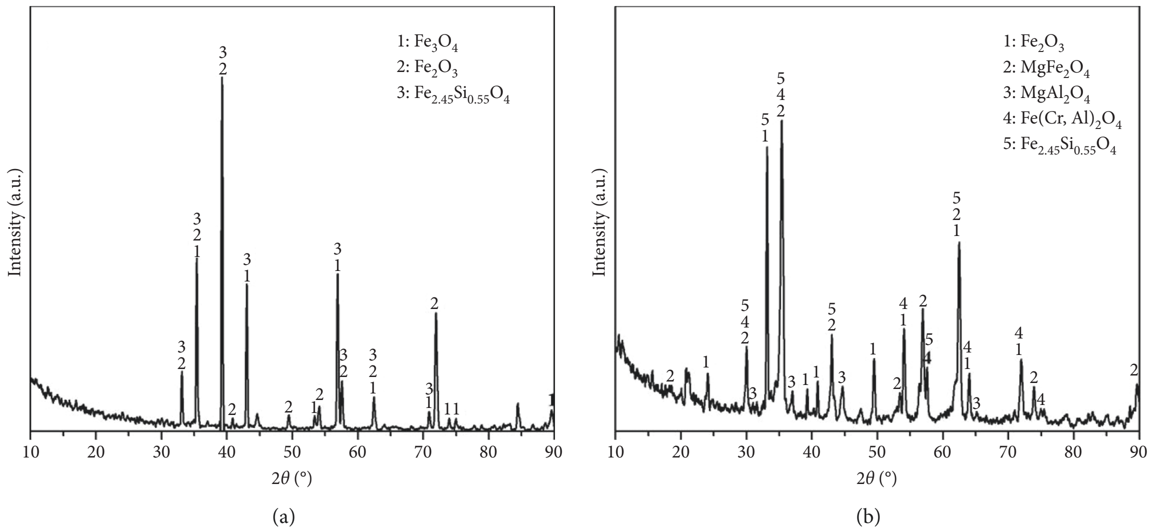

FIGURE 4: XRD patterns of (a) uncoated sample and (b) coated sample.

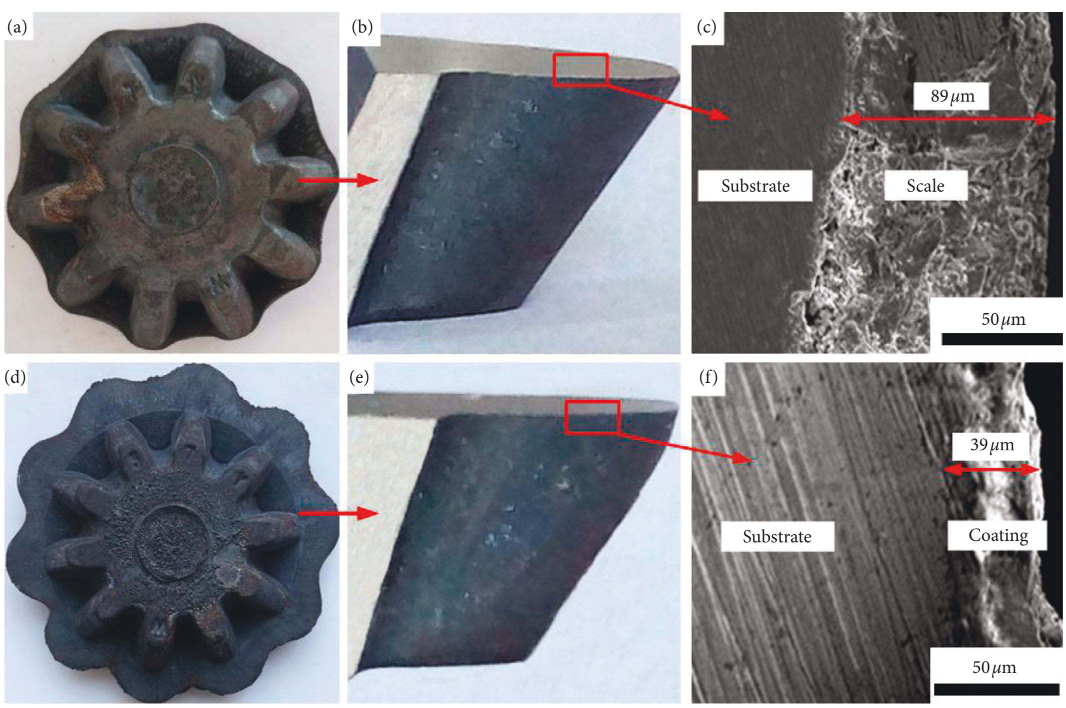

FIGURE 5: Bevel gears showing the (a) uncoated gear, (b) uncoated teeth, (c) cross section of uncoated gear forgings, (d) coated gear, (e) coated teeth, and (f) cross section of coated gear forgings.

the surface of the coated gear is 39 μm. The hot forging process of the bevel gear was simulated by means of DEFORM-3D. Through an analysis of the normal pressure and the flow velocity in a forming process of a bevel gear, the loads on the coating were shown.

Figure 7 shows a time curve of the normal pressure and velocity at top and side of a gear tooth. When running to 0.0026 s, the tooth side is in contact with die. The flow velocity of the metal at the tooth side is 723 mm/s, and the flow direction of the metal is consistent with the normal direction of the mold surface. When running to 0.0393 s, the tooth top is in contact with the die. The flow velocity of the metal at the tooth top is 627 mm/s, and the flow direction begins to change from the normal direction to the parallel to the mold surface. However, the material at the tooth side flows into the free surface.

From the simulation results, we can see that the flow velocity of the metal is not zero. In the forging process, there exits the relative movement and the friction created by contact of the billet with the mold. At 1150°C, the oxide scale

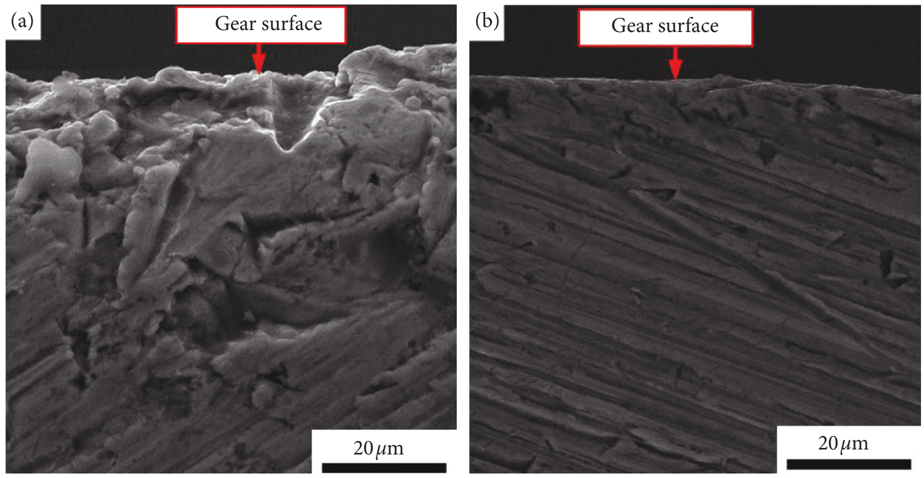

FIGURE 6: The gear surface after removing (a) the scale of the uncoated gear surface and (b) the coating of the coated gear surface.

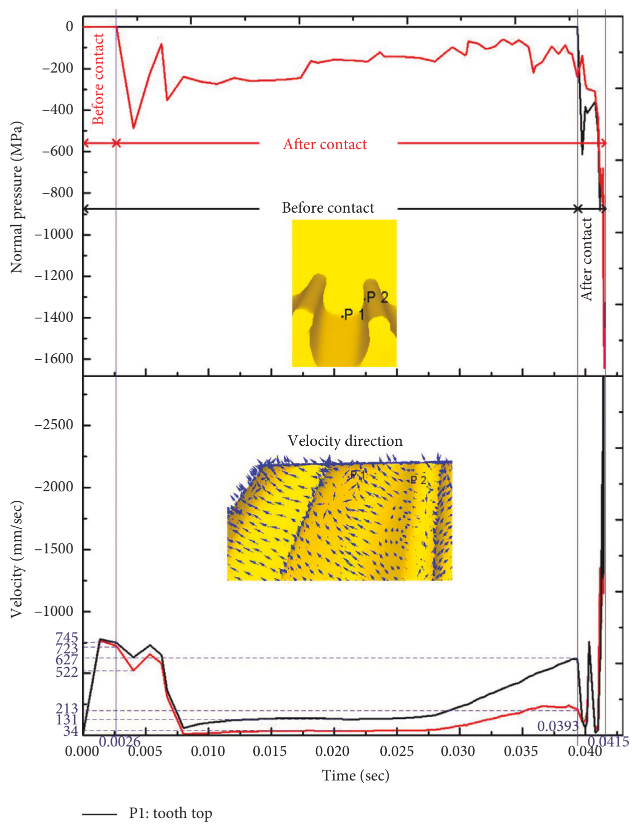

FIGURE 7: Time curves of the normal pressure and the velocity in tooth top and tooth side.

is solid and the coating is semisolid. The relationship between coating viscosity and temperature can be expressed as follows [13]:

$$\ln \eta = -0.0065T + 14.47. \quad (4)$$

The oxide scale cracks by friction and leads to oxidation of the exposed metal. Under the action of friction, the coating thickness is reduced, and the coating can be uniformly coated on the surface of the billet to prevent further oxidation of the metal.

The size of the billet is $\Phi 30\,\text{mm} \times 47\,\text{mm}$. Before forging, the surface area of the billet is $5843.4\,\text{mm}^2$. After forging, the surface area of gear forgings is $7645.3\,\text{mm}^2$. Gear forging increased the surface area of the billet by 31%. Under action of the forging stress, the oxide scale cracks because of increasing surface area and exposes the nonoxidation metal, leading to further oxidation of the billet and increasing the thickness of the oxide scale. Under the same forging stress, the slurry of coating flows and a layer of coating covered on the surface of forgings prevent further oxidation of the forgings. The coating thickness is only 43.8% of the scale thickness on the surface of noncoating forgings and the quality of the gear surface is improved, thus the dimensional accuracy and surface quality of gear forgings are efficiently improved.

4. Conclusions

(1) To solve the problem of high-temperature oxidation, a protective coating was prepared onto the surface of 20CrMnTi steel by the brushing technique. Holding at 1100°C for 30 min, an oxide layer of 153 μm was formed on the surface of the uncoated sample; however, no oxide layer was formed on the surface of the coated sample. The coating enhanced the antioxidation ability of 20CrMnTi steel.

(2) X-ray diffraction analyses revealed that $MgFe_2O_4$, $MgAl_2O_4$, $Fe(Cr,Al)_2O_4$, and $Fe_{2.45}Si_{0.55}O_4$ were formed on the coated sample at 1100°C, which increases the density of coating and effectively reduces the diffusion speed of oxygen.

(3) The billet was heated to 1150°C and then subjected to be forged in a friction press to form a certain size of bevel gear. After hot forging, the thickness of the scale on the uncoated surface is 89 μm while the thickness of film on the coating surface is 39 μm. After removing the oxide scale or coating film, the surface of the uncoated gear is rough and the surface of the coated gear is very smooth. When applied on the surface of the steel, such a coating material can not only enhance the dimensional accuracy but also improve the surface quality of forged gears.

(4) In the forging process, there is friction on the surface between billet and die and the surface area of billet will increase. The oxide scale will crack and lead to further oxidation of the metal of the uncoated billet. But for the coating billet, the coating thickness is reduced and the coating slurry can be uniformly adhered on the surface of the billet to prevent further oxidation of the metal. So, the coating can effectively improve the dimensional accuracy and the surface quality of gear forgings.

Data Availability

The data used to support the findings of this study are available from Nana Han upon request.

Conflicts of Interest

The authors declare that there are no conflicts of interest regarding the publication of this paper.

References

[1] R. Balendra, "Economic considerations in die-form compensation for nett-forming," *Journal of Materials Processing Technology*, vol. 115, no. 2, pp. 260–263, 2001.

[2] Z. B. He, G. N. Chu, J. Zhang et al., "Development of forging technology," *Journal of Plasticity Engineering*, vol. 15, no. 4, pp. 13–18, 2008.

[3] F. X. Tian, "Design of tooth form of die for precision forging spur gear," *Forging and Stamping Technology*, vol. 2, pp. 57–59, 1998.

[4] X. M. Xia, M. J. Sun, W. Wang et al., "Industry experiment and effect of oxidation resistance coating for steel slab," *Baosteel Technical Research*, vol. 6, no. 4, pp. 11–15, 2012.

[5] M. Kitayama and H. Odashima, "Method for preventing decarburization of steel materials," US Patent 4227945, 1980.

[6] X. Wang, L. Wei, X. Zhou, X. Zhang, S. Ye, and Y. Chen, "A superficial coating to improve oxidation and decarburization resistance of bearing steel at high temperature," *Applied Surface Science*, vol. 258, no. 11, pp. 4977–4982, 2012.

[7] X. Shan, L. Q. Wei, X. M. Zhang et al., "A protective ceramic coating to improve oxidation and thermal shock resistance on CrMn alloy at elevated temperatures," *Ceramics International*, vol. 41, no. 3, pp. 4706–4713, 2015.

[8] M. H. Chen, W. B. Li, M. L. Shen, S. Zhu, and F. Wang, "Glass coatings on stainless steels for high-temperature oxidation protection: mechanisms," *Corrosion Science*, vol. 82, pp. 316–327, 2016.

[9] X. H. Yang, X. Zhou, S. T. Wang et al., "Study on mechanism of Mg-Al-O high temperature protective coating for Ni-containing alloy steel," *Paint and Coatings Industry*, vol. 46, no. 1, pp. 1–7, 2016.

[10] G. Fu, L. Wei, X. Shan et al., "Influence of a Cr_2O_3 glass coating on enhancing the oxidation resistance of 20MnSiNb structural steel," *Surface and Coatings Technology*, vol. 294, pp. 8–14, 2016.

[11] X. Zhou, S. F. Ye, H. W. Xu, P. Liu, X. J. Wang, and L. Q. Wei, "Influence of ceramic coating of MgO on oxidation behavior and descaling ability of low alloy steel," *Surface and Coatings Technology*, vol. 206, no. 17, pp. 3619–3625, 2012.

[12] X. Shan, L. Q. Wei, P. Liu et al., "Influence of CoO glass-ceramic coating on the anti-oxidation behavior and thermal shock resistance of 200 stainless steel at elevated temperature," *Ceramics International*, vol. 40, no. 8, pp. 12327–12335, 2014.

[13] J. X. Zhu, S. L. Liu, and L. Q. Zhang, "High-temperature resistant coating for stainless steel," *Materials Protection*, vol. 30, no. 9, pp. 38–42, 2000.

[14] F. Wei and Y. Fu, "High temperature deformation behavior and constitutive modeling for 20CrMnTiH steel," *Materials & Design*, vol. 57, pp. 465–471, 2014.

[15] A. Chattopadhyay and T. Chanda, "Role of silicon on oxide morphology and pickling behaviour of automotive steels," *Scripta Materialia*, vol. 58, no. 10, pp. 882–885, 2008.

[16] A. B. Woodland and R. J. Angel, "Crystal structure of a new spinelloid with the wadsleyite structure in the system Fe_2SiO_4-Fe_3O_4 and implications for the Earth's mantle," *American Mineralogist*, vol. 83, no. 3-4, pp. 404–408, 1998.

[17] Y. Q. Liu, *Phase Diagrams in Silicate Ceramics*, Chemical Industry Press, Beijing, China, 1st edition, 2011.